

# Measurements of vector magnetic field using multiple electromagnetically induced transparency resonances in Rb vapor

Kevin Cox,<sup>1</sup> Valery I. Yudin,<sup>2,3,4</sup> Alexey V. Taichenachev,<sup>2,3,4</sup> Irina Novikova,<sup>1</sup> and Eugeny E. Mikhailov<sup>1</sup>

<sup>1</sup>*Department of Physics, College of William&Mary, Williamsburg, Virginia 23185, USA*

<sup>2</sup>*Institute of Laser Physics SB RAS, Novosibirsk 630090, Russia*

<sup>3</sup>*Novosibirsk State Technical University, Novosibirsk 630092, Russia*

<sup>4</sup>*Novosibirsk State University, Novosibirsk 630090, Russia*

(Dated: October 28, 2018)

We study dependence of electromagnetically induced transparency (EIT) resonance amplitudes on the external magnetic field direction in a  $lin||lin$  configuration in  $^{87}\text{Rb}$  vapor. We demonstrate that all seven resolvable EIT resonances exhibit maxima or minima at certain orientations of the laser polarization relative to the wave vector and the magnetic field. This effect can be used for development of a high-precision vector EIT magnetometer.

PACS numbers: 42.50.Gy, 32.70.Jz, 32.60.+i, 07.55.Ge

The ability to measure magnetic field with high precision and good spatial resolution benefits many applications. For example, detection of weak magnetic field distribution gives a new non-invasive diagnostic method for heart and brain activities, allows identification of defects in magnetizable coatings and films, and can possibly be used for a non-demolishing readout of stored memory domains. Many magnetic sensors available today, such as SQUIDS (superconducting quantum interference devices) [1], spin-exchange relaxation-free (SERF) magnetometers [2, 3], and various optical pumping magnetometers [4] are sensitive only to the magnitude of the magnetic field. These magnetometers lose valuable information about magnetic field direction and can allow reduced accuracy due to “heading error” in some systems [5].

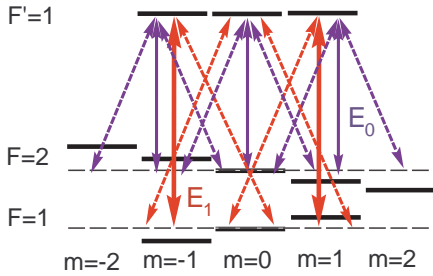


FIG. 1. Possible EIT  $\Lambda$  systems for different magnetic field orientations: solid arrows show  $\Delta m = 0$  transitions, and dashed arrows show  $\Delta m = \pm 1$  transitions.

The application of coherent optical effects, such as electromagnetically induced transparency (EIT) [6] for magnetic field detection offers exciting perspective for development of high-precision miniature magnetometers [7–12]. EIT resonances are associated with the preparation of atoms into a coherent non-interacting (dark) superposition of two metastable states of an atom (such as two Zeeman or hyperfine sublevels of the electronic ground state of an alkali metal atom) under the com-

bined interaction of two optical fields  $E_{0,1}$  in two-photon Raman resonance in a  $\Lambda$  configuration. The resulting ultra-narrow (down to a few tens of Hz [13, 14]) transmission peaks can be used to measure, *e.g.*, a frequency difference between two hyperfine energy levels in Rb or Cs without use of microwave interrogation, making this method particularly attractive for development of miniature atomic clocks [15, 16] and magnetometers [10]. In the latter case, the magnitude of a magnetic field can be deduced from the spectral position of an EIT resonance in a  $\Lambda$  link formed between magnetic field-sensitive Zeeman sublevels. However, this method is not sensitive to the direction of the magnetic field vector  $\vec{B}$ .

Several publications suggested that the information about  $\vec{B}$  direction can be extracted by analyzing relative intensities of various EIT peaks [17, 18]. Yudin *et al.* [19] showed that a recently studied  $lin||lin$  configuration is a promising candidate for EIT atomic clock applications [20–23]. The amplitude of the magneto-insensitive EIT resonance is sensitive to the magnetic field direction and has a universal maximum when the laser polarization vector,  $\vec{E}$ , is orthogonal to the plane formed by the magnetic field vector,  $\vec{B}$ , and laser wave vector,  $\vec{k}$ . Thus, measuring the resonance amplitude while rotating the laser polarization should provide information about magnetic field direction. Moreover, since this effect is based only on fundamental symmetries of the problem, corresponding measurement procedure does not require any assumptions regarding the details of the experimental arrangements (such as laser power and detuning).

In this Brief Report we explore the possibility to simultaneously measure magnetic field magnitude and direction by recording both the spectral positions and relative amplitudes of multiple Zeeman-shifted EIT resonances that occur for a bichromatic linearly polarized laser field interacting with  $^{87}\text{Rb}$  atomic vapor placed in an external uniform magnetic field. In this case EIT resonance conditions are fulfilled in various possible  $\Lambda$ -systems formed between Zeeman sublevels of two hyperfine states of Rb

atoms, shown in Fig. 1, for several two-photon detunings  $\Delta_{\text{HFS}} + n\mu_B g B$ , where  $n = 0, \pm 1, \pm 2, \pm 3$ ,  $\Delta_{\text{HFS}}$  is the hyperfine splitting,  $g$  is the gyromagnetic ratio,  $\mu_B$  is the Bohr magneton. Other parameters of each EIT peak (amplitude, width) strongly depend on the mutual orientation of magnetic field, light polarization and wavevector directions that define Rabi frequencies of optical fields for each  $\Lambda$  link according to the selection rules. However, a universal intrinsic symmetry of this problem [19] predicts that all EIT resonance amplitudes must exhibit local maxima or minima for two orientations of light polarization  $\vec{E}$ : when  $\vec{E}$  is orthogonal to the  $\vec{B}-\vec{k}$  plane, and when it lays within that plane. Here we confirm (both experimentally and by using exact numerical calculations) that such universal extrema exist for all observed EIT resonances, even though their characteristic strength (maximum vs minimum) will change depending on direction of the magnetic field. Since the exact angular position of such extrema [19] does not depend on parameters of the laser (such as laser intensity), they should provide accurate information about magnetic field orientation.

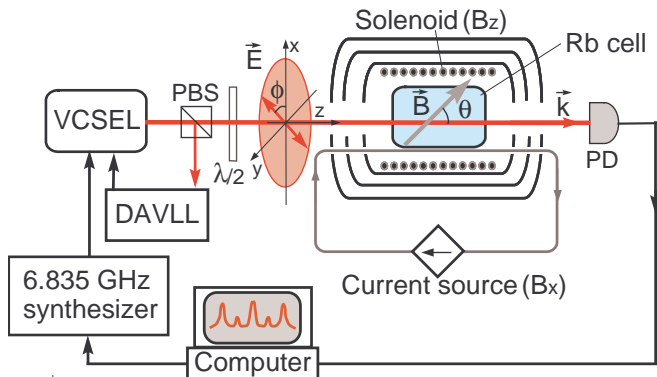


FIG. 2. (Color online) Schematic of the experimental setup. See text for abbreviations.

Our experimental arrangements (see Fig. 2) are similar to those used for miniature EIT-based magnetometers [10] (although most components are not miniaturized). The details of the construction and operation of our experimental apparatus are given in [23, 25]. A temperature-stabilized vertical cavity surface-emitting diode laser (VCSEL) was current-modulated at  $\nu_m = 6.8347$  GHz with the laser carrier frequency tuned at  $5S_{1/2}F = 2 \rightarrow 5P_{1/2}F' = 1$  transition and the first modulation sideband resonant with  $5S_{1/2}F = 1 \rightarrow 5P_{1/2}F' = 1$  transition (see Fig. 1) using a dichroic-atomic-vapor laser lock (DAVLL) [26]. The intensity ratio between the sideband and the carrier was adjusted by changing the modulation power sent to the VCSEL, while the modulation frequency (and consequently the two-photon detuning of two EIT fields) was controlled by a home-made computer-controlled microwave source operating at 6.835 GHz [23]. During this experiment we kept the sideband to carrier ratio equal to 60%, since this allows us to cancel the first order power shift in this setup [22, 23].

The laser beam with maximum total power  $120 \mu\text{W}$  and a slightly elliptical Gaussian profile [1.8 mm and 1.4 mm full width half maximum (FWHM)], traverses a cylindrical Pyrex cell (length 75 mm; diameter 22 mm) containing isotopically enriched  $^{87}\text{Rb}$  vapor and 15 Torr of Ne buffer gas, mounted inside a three-layer magnetic shielding and actively temperature-stabilized at  $47.3^\circ\text{C}$ . To control the polarization of the laser before the cell, the beam passes a polarizing beam splitter (PBS) and then a half-wave plate ( $\lambda/2$ ) that rotates the direction of polarization in  $x-y$  plane. The polarization angle  $\phi$  is defined as an angle between the polarization direction and a vertical  $x$  axis.

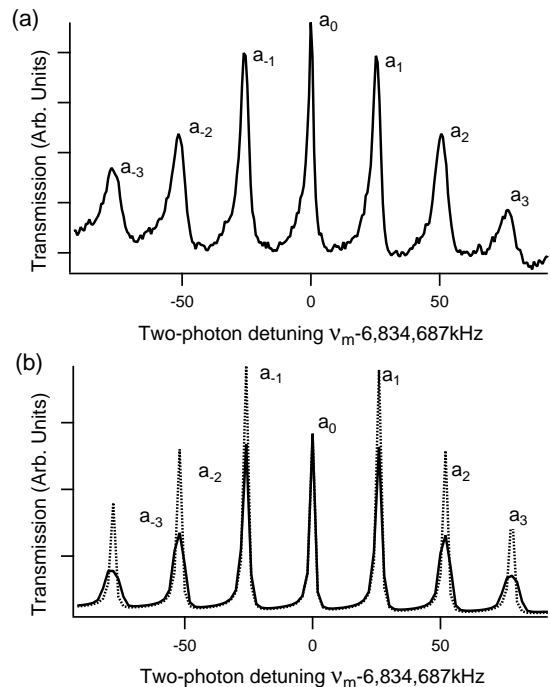


FIG. 3. (a) Sample experimental EIT resonances for  $\theta = 90^\circ$  and  $\phi = 60^\circ$ , with angles defined in Fig. 2. (b) Matching theoretical calculations for a perfectly homogeneous magnetic field (dotted line) and taking into account transverse gradient from the wire (solid line).

A solenoid inside magnetic shield produces magnetic field  $B_z$  parallel to  $\vec{k}$ , while a straight wire parallel to the light propagation direction produces a transverse component  $B_x$ . Special care was taken to align the laser beam strictly parallel to the  $B_x$  generating wire to avoid variation of the  $B$  field along the beam propagation direction. Calibrated, simultaneous adjustment of current in both the solenoid and the wire allowed us to change the direction of the magnetic field  $\theta$  (measured from the  $z$ -axis) without changing the magnitude of  $B$  and associated 26 kHz Zeeman splitting.

During experiments, for a given angles  $\theta$  and  $\phi$  we recorded laser field transmission as a function of two-photon detuning by scanning the laser's microwave mod-

ulation frequency  $\nu_m$  around the  $^{87}\text{Rb}$  hyperfine splitting. A sample spectrum Fig. 3(a) shows seven EIT peaks that are labeled according to their Zeeman shift: the magneto-insensitive peak at  $\nu_m = \Delta_{\text{HFS}}$  is labeled  $a_0$ , while peaks separated by  $\pm$  one, two and three Zeeman splitting are  $a_{\pm 1}$ ,  $a_{\pm 2}$ , and  $a_{\pm 3}$  respectively. Amplitudes of each EIT peak were extracted from the Lorentzian fit and then normalized to the maximum  $a_0$  amplitude for each angle  $\theta$ .

Our experimental results are supported by the numerical calculations for complete hyperfine and Zeeman structure of Rb atoms based on the standard density-matrix approach (see, *e.g.*, Ref. [24]) under assumptions of low saturation and total collisional depolarization of the excited state. The parameters used in the calculations matched the experimental conditions: total intensity of the two fields  $I_1 + I_0 = 0.5 \text{ mW/cm}^2$  and  $I_1/I_0 = 0.6$ , optical transition linewidth  $\gamma = 100 \text{ MHz}$ , ground state decoherence rate  $\gamma_0 = 500 \text{ Hz}$ , and Zeeman splitting  $\mu_B g B = 26 \text{ kHz}$ .

Fig. 3(b) shows a calculated EIT spectrum. To achieve good agreement with the experiment we took into account a transverse magnetic field gradient created by the straight wire that was characterized experimentally in our previous work [28]. Such variation of the magnetic field produced small differential shifts of the EIT resonance positions across the laser beam cross-section, that resulted in broadening of the magneto-sensitive peaks and change in their relative amplitudes. This effect was taken into account in numerical calculations by averaging the results over 25-point rectangular grid across the beam.

Fig. 4 shows both experimental data and theoretical calculations for the amplitudes of all seven EIT resonances as functions of laser polarization angle  $\phi$  for two different angles  $\theta$ . The strongest dependence on light polarization were observed for mostly transverse magnetic fields  $\vec{B} \perp \vec{k}$  [see Figs. 4(a,c)]. According to the selection rules, only optical transitions with  $\Delta m_F = 0$  are possible for  $\vec{B} \parallel \vec{E}$  ( $\phi = 0^\circ$  and  $\theta = 90^\circ$ ). Thus, only  $a_{-2}$  and  $a_2$  EIT resonances appear at the two-photon detunings  $\Delta_{\text{HFS}} \pm 2g\mu B$  (transition  $F = 1, m_F = 0 \rightarrow F' = 1, m_F = 0$  is forbidden due to symmetry); all other EIT peaks vanish. Similarly, at  $(\vec{B} \perp \vec{k}) \perp \vec{E}$  ( $\phi = 90^\circ$  and  $\theta = 90^\circ$ ), only transitions with  $\Delta m_F = \pm 1$  are allowed, resulting in only three EIT resonances at  $\Delta_{\text{HFS}}$  and  $\Delta_{\text{HFS}} \pm 2g\mu B$ . At any other intermediate angle, the same two Zeeman sublevels can participate in more than one  $\Lambda$  systems, resulting in constructive or destructive interference depending on their Clebsch-Gordan coefficients. This makes calculations of EIT resonance amplitudes more complicated. Furthermore, when there is a significant longitudinal component of the magnetic field present, the amplitude of EIT resonance become less sensitive to the light polarization, as shown in Figs. 4(c,d). However, there are still clear extrema at  $\phi = 0$  and  $\phi = 90^\circ$  for all EIT resonances. We experimentally observed this to be true for any direction of the magnetic

field. The only exception is longitudinal magnetic field ( $\vec{B} \parallel \vec{k}$ ) since, as expected, no polarization dependence is observed.

In the ideally symmetric situation, the amplitudes of resonances with the same value but opposite detunings (*e. g.*,  $a_1$  and  $a_{-1}$ ) should be identical. However, complex hyperfine and Zeeman structure of the excited state causes a slight asymmetry of EIT resonances (see Fig. 3) for nominal zero optical (one-photon) detuning. Combined with a relatively small (compared to the resonance linewidth) Zeeman shift this asymmetry leads to a small difference in resonance amplitudes for “positive” and “negative” peaks, which is more noticeable in our experiment for small angles  $\theta$  [see Fig. 4(b)]. The resonance asymmetry can be reduced by optimizing the laser detuning [22] and by operating at higher magnetic fields.

Measuring extrema positions of resonance amplitudes vs light polarization rotation angle dependence allows one to find the plane in which the magnetic field vector lies. For a complete measurement of magnetic field direction, one must take two independent measurements of two such planes, and then determine the direction of  $\vec{B}$  from their intersect. This can be done, for example, by repeating the measurement for two different light propagation directions in the  $x-z$  plane [19]. Alternatively, an additional magnetic field of known magnitude and direction controllably “rotate” the total magnetic field for the second measurement. However, for well-characterized experimental parameters the dependence of resonance amplitudes on polarization angle  $\phi$  are unique for every magnetic angle  $\theta$ , forming a magnetic direction “fingerprint”. Such a fingerprint may allow a simplified procedure for extracting  $\vec{B}$  information. Because of the symmetry of the  $lin \parallel lin$  polarization configuration, the same fingerprint will be obtained for two possible direction combinations  $\theta$  and  $\pi - \theta$  with respect to the  $z$  axis. This degeneracy can be lifted by sending an elliptically polarized light, which breaks this symmetry and makes either positive or negative resonances stronger depending on the magnetic field direction.

This measurement procedure can also be used to produce high-resolution maps of vector magnetic fields when used in combination with a recently-demonstrated magnetic field imager [28], as long as light transmission across the laser beam is spatially resolved. Since the EIT resonance positions depends on the Zeeman shifts of atomic sublevels, the resonances will occur at different two-photon detunings for different spacial locations in the case of a spacially varying magnetic field. Recording a series of such images for various two-photon frequencies for a particular EIT resonance can create a spatial map of the magnetic field magnitude. Repeating such measurements for several orientations of the laser polarization and finding an extremas in resonance amplitude provides additional information about variations in the direction of the magnetic field.

In summary, we systematically studied dependence of multiple EIT resonances’ on relative orientation of mag-

netic field and laser polarization in the  $lin||lin$  configuration using a current-modulated VCSEL on the  $D_1$  line of  $^{87}\text{Rb}$ . We demonstrated that all observed EIT resonances can be used to extract complete information about magnetic field vector with improved sensitivity to directionality. These findings can be used to implement a sensitive small scale vector magnetometer and/or magnetic field imager with good spatial resolution.

The authors would like to thank S. Zibrov, A. S. Zi-

brov and V. L. Velichansky for useful discussions. This research was supported by the National Science Foundation grant PHY-0758010. A.V.T and V.I.Yu. were supported by RFBR (grants 09-02-01151, 10-02-00406, 11-02-00775, 11-02-00786, 11-02-01240), DFG/RFBR (grant 10-02-91335), Russian Academy of Science, Presidium SB RAS, and by federal program “Scientific and pedagogic personnel of innovative Russia 2009-2013”. K.C. acknowledges support from the Virginia Space Grant Consortium through Undergraduate Research Scholarship.

- 
- [1] J. Clarke, in *SQUID Sensors: Fundamentals, Fabrication, and Applications*, edited by H. Weinstock (Kluwer Academic, The Netherlands, 1996), pp. 1-62.
- [2] I. K. Kominis, T. W. Kornack, J. C. Allred, and M. V. Romalis, *Nature* **422**, 596 (2003).
- [3] D. Budker, M. V. Romalis, *Nature Phys.* **3**, 227 (2007).
- [4] E. B. Alexandrov and V. A. Bonch-Bruевич. *Opt. Eng.* **31**, 711 (1992).
- [5] J.E. Lenz, *Proc. IEEE* **78**, 973 (1990).
- [6] M. Fleischhauer, A. Imamoglu J. P. Marangos, *Rev. Mod. Phys.* **77**, 633 (2005).
- [7] M. Fleischhauer and M. O. Scully, *Phys. Rev. A* **49**, 1973 (1994).
- [8] C. Affolderbach, M. Stähler, S. Knappe and R. Wynands, *Appl. Phys. B* **75**, 605 (2002).
- [9] H. Xia, A. Ben-Amar Baranga, D. Hoffman, and M. V. Romalis, *Appl. Phys. Lett.* **89**, 211104 (2006).
- [10] V. Shah, S. Knappe, P. D. D. Schwindt, and J. Kitching, *Nature Photonics* **1**, 649-652 (2007).
- [11] M. P. Ledbetter, I. M. Savukov, D. Budker, V. Shah, S. Knappe, J. Kitching, D. J. Michalak, S. Xu, and A. Pines, *Proc. Nat. Acad. Sci.* **105**, 2286-2290 (2008).
- [12] G. Bison, N. Castagna, A. Hofer, P. Knowles, J.-L. Schenker, and A. Weis, *Appl. Phys. Lett.* **95**, 173701 (2009).
- [13] D. Budker, V. Yashchuk, and M. Zolotarev, *Phys. Rev. Lett.* **81**, 5788 (1998).
- [14] M. Erhard and H. Helm, *Phys. Rev. A* **63**, 043813 (2001).
- [15] J. Vanier, *Appl. Phys. B* **81**, 421 (2005).
- [16] S. Knappe, P. D. D. Schwindt, V. Shah, L. Hollberg, J. Kitching, L. Liew, and J. Moreland, *Opt. Express* **13**, 1249-1253 (2005).
- [17] R. Wynands, A. Nagel, S. Brandt, D. Meschede, and A. Weis, *Phys. Rev. A* **58**, 196 (1998).
- [18] H. Lee, M. Fleischhauer, and M. O. Scully, *Phys. Rev. A* **58**, 2587 (1998).
- [19] V. I. Yudin, A. V. Taichenachev, Y. O. Dudin, V. L. Velichansky, A. S. Zibrov, and S. A. Zibrov, *Phys. Rev. A* **82**, 033807 (2010).
- [20] A. V. Taichenachev, V. I. Yudin, V. L. Velichansky, and S. A. Zibrov, *JETP Lett.* **82**, 398 (2005).
- [21] E. Breschi, G. Kazakov, R. Lammegger, G. Miletì, B. Matsov, and L. Windholz, *Phys. Rev. A* **79**, 063837 (2009).
- [22] S. A. Zibrov, I. Novikova, D. F. Phillips, R. L. Walsworth, A. S. Zibrov, V. L. Velichansky, A. V. Taichenachev, and V. I. Yudin, *Phys. Rev. A* **81**, 013833 (2010).
- [23] E. E. Mikhailov, T. Horrom, N. Belcher, and I. Novikova, *J. Am. Opt. Soc. B* **27**, 417 (2010).
- [24] A. V. Taichenachev, V. I. Yudin, R. Wynands, M. Stähler, J. Kitching, and L. Hollberg, *Phys. Rev. A* **67**, 033810 (2003).
- [25] N. Belcher, E. E. Mikhailov, and I. Novikova, *Am. J. Phys.*, **77**, 988 (2009).
- [26] V. V. Yashchuk, D. Budker, and J. R. Davis, *Rev. Sci. Instr.* **71**, 341-346 (2000).
- [27] A. V. Taichenachev, V. I. Yudin, R. Wynands, M. Stähler, J. Kitching, and L. Hollberg, *Phys. Rev. A* **67**, 033810 (2003).
- [28] E. E. Mikhailov, I. Novikova, M. D. Havey, and F. A. Narducci, *Opt. Lett* **34**, 3529 (2009).

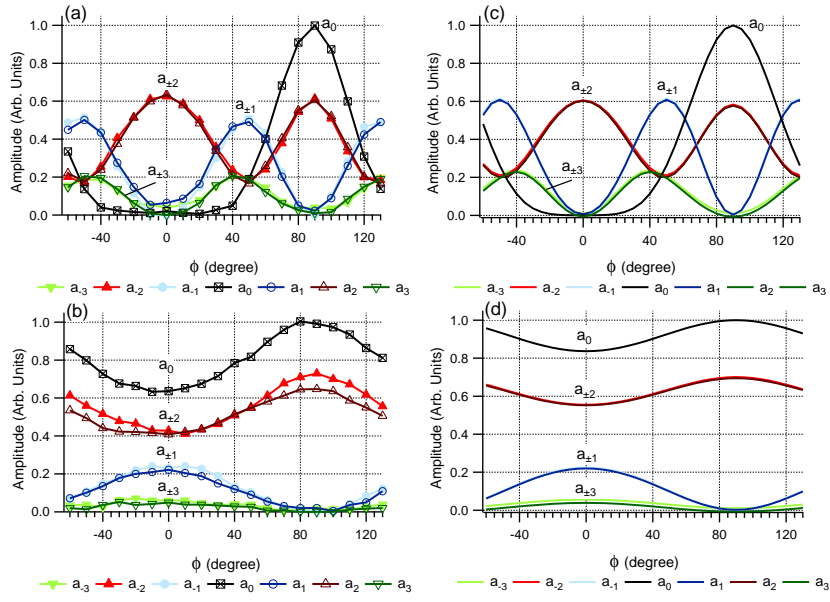


FIG. 4. Experimental (a,b) and theoretical (c,d) dependence of the EIT resonance amplitudes on polarization angle  $\phi$  for magnetic field angles  $\theta = 90^\circ$  (top row) and  $\theta = 15^\circ$  (bottom row).